Reports

Far-Infrared Observations of the Night Sky

Abstract. *We have flown a telescope cooled to liquid-helium temperatures and made far-infrared observations of the night sky. A gallium-doped germanium detector, sensitive from 5.2 to 130 micrometers, detected a minimum signal of 10^{-9} watt per square centimeter per steradian referred to 100 micrometers. The origin of this signal can be instrumental, atmospheric, interplanetary, or interstellar. We can place a firm upper limit on the color temperature of a dilute cosmic background flux.*

We have carried out observations of the night sky in the spectral range from 5.2 to 1300 μm by means of a rocket-borne telescope. The telescope (*1*) had a field of view of 5°, a focal ratio *f* of 0.9, and an aperture of 17 cm. The telescope, cooled to liquid-helium temperatures, was carried to an altitude of 170 km at 20 : 30 M.S.T. on 29 February 1968 by an Aerobee rocket launched from White Sands, New Mexico. We now discuss observations made in the spectral range from 5.2 to 130 μm. Shivanandan *et al.* (*2*) have presented data in the submillimeter range.

All of the detectors were mounted in a common integrating cavity. The entrance to the cavity defined a common field of view of 5° and was covered by a filter set consisting of a wire mesh and a germanium interference filter. These filters limited the response of the detectors at long and short wavelengths, that is, at 1300 and 5.2 μm, respectively.

An attitude-control system incorporating a roll-stabilized platform pointed the telescope in a set of predetermined directions. The insert (Fig. 1) shows the regions of the sky scanned by the telescope during the flight. During the observations the angle between the axis of the telescope and the horizon was always greater than 25°.

One serious technical problem arose during the flight. Because of a malfunction in one of the valves designed to control the pressure (temperature) of the liquid helium, the entire telescope cooled down. By the end of the observations, the telescope temperature was 2.4°K. As a result, the sensitivity of the photoconductor-preamplifier assembly decreased by an order of magnitude. We know this from both in-flight calibration and post-flight measurements made when the payload was recovered.

A Perkin-Elmer 301 spectrophotometer was used to measure the spectral response of the detectors. The system was calibrated absolutely by placing a blackbody over the entrance aperture of the telescope. To test the blackness of the emitting surface, a cavity was constructed by placing a perforated copper plate over the emitting surface. The signal generated by the radiation coming through the perforations was compared to the signal obtained from exposure to the full-area blackbody. The ratio of these two signals was equal within experimental error to the ratio of the exposed areas. This indicates that the efficiency of the emitting surface was near 100 percent. One of the gallium-doped germanium detectors received light that had passed through only the germanium and wire-mesh filters. A second gallium-doped detector received light which had passed through an additional NaCl crystal 2 mm thick. Sodium chloride was chosen as a filter material because of its high attenuation at 63 μm where there is a strong atmospheric emission line due to atomic oxygen (*3*). The gallium-doped detector without the sodium chloride filter had a peak system sensitivity *S* of 3×10^{-9} watt cm^{-2} sr^{-1}. The gallium-doped detector with the sodium chloride filter, Ge : Ga (NaCl), had a peak sensitivity of 2.5×10^{-11} watt cm^{-2} sr^{-1}; its spectral response is shown in Fig. 2. A copper-doped germanium detector was also flown but it seemed to give erratic response during flight.

We obtained a very definite signal from the Ge : Ga (NaCl) detector when the telescope was pointed near the zenith. Because of the detector's broad spectral response, this signal can be interpreted in a number of ways. If the radiation is assumed to have a wavelength near 100 μm, the required incident flux is smallest and amounts to 10^{-9} watt cm^{-2} sr^{-1}. There are several possible sources of this radiation.

1) *Scattered light from Earth.* Figure 1 shows a plot of the observed signal strength as a function of zenith angle. The solid curve shows the expected shape if all the response is due to scattered radiation from Earth. This curve is based on laboratory measurements of the light-baffling properties of the telescope. More total scattered radiation was observed in flight than would be expected on the basis of the laboratory measurements.

Since the response of the Ge : Ga detector to the emission spectrum from Earth peaks at about 70 μm whereas the laboratory measurements were made with visible light, one would expect a different amount of scattering at the longer wavelengths. This is what was observed. The solid curve (Fig. 1) has been shifted upward in absolute intensity by a factor of 10. The observations fit the shape of the laboratory curve for large zenith angles but are definitely higher than the curve near $\Phi = 0$. It is therefore unlikely that the signal obtained near the zenith is due entirely to scattered emission from Earth.

2) *Heating of the radiation baffles.* During the observations the front of the telescope was shielded from direct radiation from Earth by two concentric sets of beryllium-copper baffles (*1*) made of thin strips (0.01 cm thick) 5 cm wide and 20 cm long. The outer baffles extended about 5 cm farther than the inner ones. In this way the inner baffles and the interior of the telescope were shielded from direct radiation coming from Earth and from the skin of the rocket. If all of the baffles were in good thermal contact with the liquid-helium reservoir, even direct radiation from Earth could not heat the baffles appreciably. However, if one or more of the strips had poor thermal contact, they could have become hot enough to be detected by the

gallium-doped detectors toward the end of the flight. Therefore, the increased signal observed from the zenith near the end of the flight might be due to heating of the baffles. The heating would have occurred when the telescope pointed close to the horizon ($\Phi = 79°$).

Preflight signal levels detected by the Ge : Ga detector show that the outer set of baffles was warmer than the inner set. It is possible that radiation from these outer baffles may have found its way through the inner set to produce a false signal in flight.

3) *Atmospheric emission.* Several investigators have predicted far-infrared emission from the upper atmosphere (*3, 4*). They have pointed out that the bulk of the expected radiation above 100 km would arise from a transition within the ground state of atomic oxygen. This should give rise to a strong flux at 63 μm. During our flight the telescope pointed toward the zenith while at different altitudes. Roughly twice as much signal is seen at the lower altitudes. If the radiation were due to the transition at 63 μm, one would expect an intensity ratio of at least 16 to 1 between 170 and 120 km (*5*). This leads us to conclude that the signals are not due entirely to atomic O (63 μm). However, the increase in the signal seen at lower altitudes may be due to O (63 μm), in which case its intensity at 120 km is 8×10^{-9} watt cm^{-2} sr^{-1}.

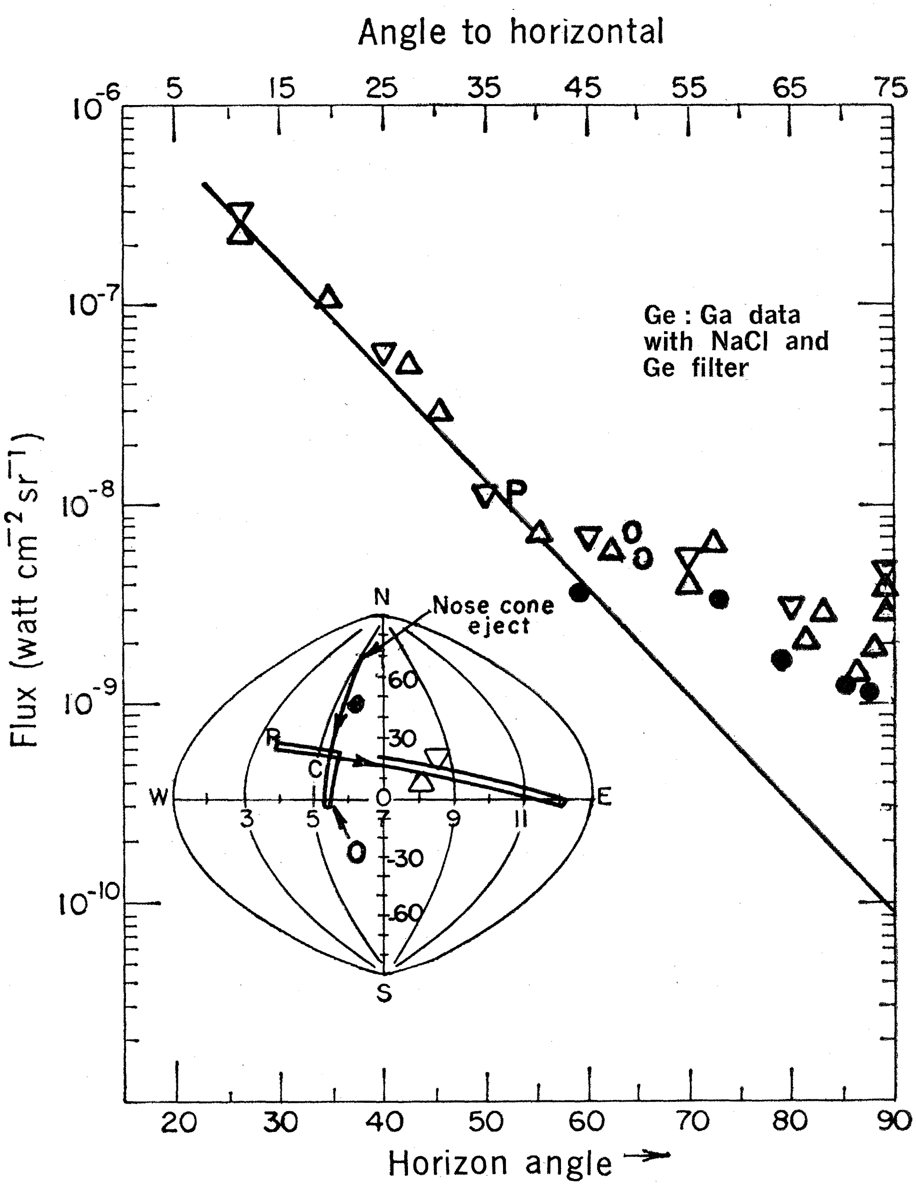

Fig. 1. Observed signal strength as a function of the angle between the axis of the telescope and the horizon. The solid line gives the predicted shape of the scattered emission from Earth based on laboratory measurements of the light-baffling characteristics of the telescope. The line has been fitted to the observations for large Φ. For small Φ the observed intensity is higher than that expected from scattered emission from Earth. The inset (lower left) shows the regions of the sky scanned and scan paths during the flight. The Orion Nebula, Pleiades, and Crab Nebula are marked by *O*, *P*, and *C*. Scans $\triangle$ (at ~ 170 km) and ∇ (at ~ 120 km) are along the ecliptic; Φ, the zenith angle, is complementary to the "angle to horizontal."

4) *Zodiacal light.* Since the ecliptic was near the zenith during the observations, one must consider the emission of infrared radiation by zodiacal dust grains as a possible source of the observed signal. Zodiacal dust particles near Earth would have a temperature of approximately 280°K. Because the Ge : Ga (NaCl) detector responds to only a small fraction of the radiation at 280°K, the observed signal would reflect a much higher flux than theoretically predicted (*6*).

On the other hand, one might attribute the flux to thermal emission from interplanetary dust, if most of the dust at large elongation angles lies at least as far away as the asteroidal belt. Large, fluffy grains, darkened to the same extent as lunar surface material, could then emit a flux of the order of 10^{-9} watt cm^{-2} sr^{-1} between 70 and 120 μm. The amount of visible scattered light for such grains would be $\sim 10^{-9}$ watt cm^{-2} sr^{-1}.

5) *Interstellar dust.* If we assume that the signal recorded by the Ge : Ga detector is due to emission from interstellar grains, we can fit the data with grains at a temperature of 30°K and a "dust cloud emissivity" of 6×10^{-4}. If, as generally assumed, the temperature is less than 30°K, the signal would require a much larger emissivity.

6) *Microwave background.* The microwave cosmic background flux has long been conjectured to be either blackbody radiation at ~ 3°K or *n*-fold diluted radiation with a color temperature T of 3 n°K. Our observations show that, if n were greater than 6 so that the color temperature were $T > 18$°K, then the expected flux at a wavelength of < 120 μm would have exceeded the observed signal. We conclude that the cosmic background radiation, if gray, must have $T < 18$°K and $n < 6$.

Our observations are compatible with a general background flux of 1×10^{-9} watt cm^{-2} sr^{-1} referred to 100 μm. There does not appear to be an excess

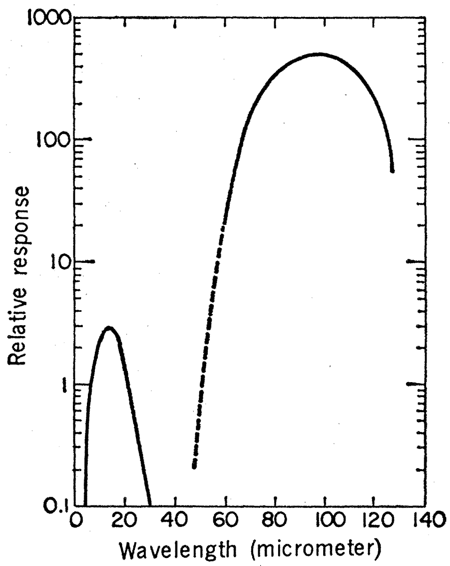

Fig. 2. Spectral response of Ge:Ga detector with wire-mesh Ge interference filter and NaCl crystal 2 mm thick.

over this amount coming from either the Orion Nebula or the Pleiades, but measurements on these sources were hindered by their proximity to the horizon. There appeared to be no strong spatial dependence associated with the flux in the small area of the sky for which contamination by scattered radiation from Earth was small. However, this zenith region was near both the ecliptic plane and the Milky Way.

If the observed signal represents a continuation of the microwave background (7), one can set an upper limit to the color temperature and a lower limit to the emissivity ε of the corresponding gray body source: $T \leq 18°K$, $\varepsilon = 1/n \geq 1/6$.

J. R. HOUCK
MARTIN HARWIT
Cornell-Syndey University Astronomy Center, Ithaca, New York 14850

References and Notes

1. M. Harwit, J. R. Houck, K. Fuhrmann, *Appl. Opt.* **8**, 473 (1969).
2. K. Shivanandan, J. R. Houck, M. Harwit, *Phys. Rev. Lett.* **21**, 1460 (1968).
3. D. R. Bates, *Proc. Phys. Soc. London* **B64**, 805 (1951).
4. A. Dalgarno, *Phil. Trans. Roy. Soc. London* in press.
5. We compute this ratio on the basis of unpublished data supplied by M. Nicolet.
6. M. Harwit, *Congr. Colloq. Univ. Liege* **26**, 506 (1964); R. B. Partridge, and P. J. E. Peebles, *Astrophys. J.* **148**, 377 (1967).
7. A. A. Penzias, and R. W. Wilson, *Astrophys. J.* **142**, 419 (1965).

8. Supported by NASA contract NSR-33-010-026. We thank Mrs. J. Pipher for making the spectral calibrations of the detectors. We also thank our subcontractors, Williams Laboratories, Inc. and Pan Monitor, Inc., for assistance on the engineering problems. The efforts of J. Dunston and V. Neigh are appreciated.

20 January 1969

Moon: Two New Mascon Basins

Abstract. *Lunar gravity data and orbital photography indicate that there is a mascon basin approximately 1000 kilometers in diameter on the farside of the moon and that Mare Marginis is the flooded fraction of a mascon basin approximately 900 kilometers in diameter.*

In the course of an investigation of the association of large, localized subsurface mass concentrations (mascons) with the moon's circular maria (*1*) and the ability of such mascons to explain the differences among the lunar principal moments of inertia (*2*), we examined the existing spherical harmonic expansions of the moon's gravitational potential as one means of determining the magnitude of the mass concentrations.

We chose the expansion of Lorell and Sjogren (*3*) derived from observations of the orbits of four Lunar Orbiter spacecraft. From this description of the selenopotential we derived the distribution of mass density, on a spherical surface 300 km beneath the lunar surface, which would reproduce the spatially varying part of the moon's gravitational field. Similar distributions would hold for other depths. Figure 1 shows the resulting distribution in mass density (*4*). The diagram does show on the nearside mass concentrations at the same general locations as the more precise acceleration data of Muller and Sjogren (*1*). The widely separated mascons associated with Imbrium-Serenitatis, Orientale, and Nectaris are represented by distinct peaks which permit their masses to be estimated with an error typically less than ~ 30 percent.

In Fig. 1 there appear two large mascons which cannot be associated with those reported by Muller and Sjogren: one at the east limb near Mare Marginis and the other a very large feature near the center of the farside disk. We estimate that the masses associated with these features are about 1.4 and 2.8 times, respectively, the mass associated with Imbrium-Serenitatis. The estimate for the farside mascon is in no way dependent on the source of the additional mass in the region, but the narrow profile of the contours does imply that the mass is not dispersed over a very large area.

A unique sequence of photographs taken from Apollo 8 shows the gibbous moon from a subspacecraft selenographic longtiude of about 70°E. The photographs indicate a circular basin ~ 900 km in diameter centered at 91°E, 25°N with Mare Marginis filling the southwest corner. Zond 3 and Luna 3 photographs (*5*) also show some indication of a southwest boundary of the basin, as marked by the interface between the mare fill and the surrounding highlands. The center of the basin coincides with the peak of the mass distribution of Fig. 1, well within the limits of error, and the basin size is close to that predicted from scaling relations (*6*). [Subsequent to the submission of the first version of this report, Whitaker, who questioned the photographic evidence for the boundary of a basin centered at 91°E, 25°N, supplied details of an alternative structure that he and his colleagues discovered in the same area (*7*). It consists of a U-shaped series of scarps running southward along the 75°E meridian, eastward at approximately latitude 16°S, and northward along the 100°E meridian; it thus encloses both Mare Marginis and Mare Smythii, although it is not closed at the northern end, and Whitaker emphasized that he could discern no ridges north of 20°N. This structure, although not circular, is of about the same size as the basin we postulate.] The flooded fraction of the Marginis basin closely approximates the fraction within the nearside hemisphere. This suggests some connection between flooding physics and the gravitational influence of the earth.

Inspection of the lunar farside cartography constructed from Lunar Orbiter photographs (*8*) discloses a variety of small maria and craters, but neither collectively nor individually can these account for the mass of the farside mascon unless some mechanism very different from that causing the nearside mascons is operative. On the other hand, one can discern immediately northward of the center of the farside disk a feature which appears to be the remnant of an enormous circular basin now very heavily eroded. We originally identified this feature from the first and second editions of the Lunar Farside Chart (LFC-2 and LFC-1) and confirmed some of the escarpments from examination of in-